53. Henstridge DC, Bruce CR, Pang CP, et al. Skeletal muscle-specific overproduction of constitutively activated c-Jun N-terminal kinase (JNK) induces insulin resistance in mice. Diabetologia 2012;55:2769–2778
54. Sabio G, Kennedy NJ, Cavanagh-Kyros J, et al. Role of muscle c-Jun NH2-terminal kinase 1 in obesity-induced insulin resistance. Mol Cell Biol 2010;30:106–115
55. Okumura A, Saito T, Otani I, et al. Suppressive role of leukocyte cell-derived chemotaxin 2 in mouse anti-type II collagen antibody-induced arthritis. Arthritis Rheum 2008;58:413–421
56. Lu XJ, Chen J, Yu CH, et al. LECT2 protects mice against bacterial sepsis by activating macrophages via the CD209a receptor. J Exp Med 2013;210:5–13
57. Knudsen SH, Hansen LS, Pedersen M, et al. Changes in insulin sensitivity precede changes in body composition during 14 days of step reduction combined with overfeeding in healthy young men. J Appl Physiol (1985) 2012;113:7–15
58. Goodson NJ, Silman AJ, Pattison DJ, et al. Traditional cardiovascular risk factors measured prior to the onset of inflammatory polyarthritis. Rheumatology (Oxford) 2004;43:731–736
59. Pedersen M, Jacobsen S, Klarlund M, et al. Environmental risk factors differ between rheumatoid arthritis with and without auto-antibodies against cyclic citrullinated peptides. Arthritis Res Ther 2006;8:R133
60. Marra F, Bertolani C. Adipokines in liver diseases. Hepatology 2009;50:957–969

Diabetologia (2014) 57:878–890
DOI 10.1007/s00125-013-3149-9

ARTICLE

The effects of ezetimibe on non-alcoholic fatty liver disease and glucose metabolism: a randomised controlled trial

Yumie Takeshita · Toshinari Takamura · Masao Honda · Yuki Kita · Yoh Zen · Ken-ichiro Kato · Hirofumi Misu · Tsuguhito Ota · Mikiko Nakamura · Kazutoshi Yamada · Hajime Sunagozaka · Kuniaki Arai · Tatsuya Yamashita · Eishiro Mizukoshi · Shuichi Kaneko

Received: 11 October 2013 / Accepted: 15 November 2013 / Published online: 10 January 2014

Abstract

Aims/hypothesis The cholesterol absorption inhibitor ezetimibe has been shown to ameliorate non-alcoholic fatty liver disease (NAFLD) pathology in a single-armed clinical study and in experimental animal models. In this study, we investigated the efficacy of ezetimibe on NAFLD pathology in an open-label randomised controlled clinical trial.

Methods We had planned to enrol 80 patients in the trial, as we had estimated that, with this sample size, the study would have 90% power. The study intervention and enrolment were discontinued because of the higher proportion of adverse events (significant elevation in HbA_{1c}) in the ezetimibe group than in the control group. Thirty-two patients with NAFLD were enrolled and randomised (allocation by computer program). Ezetimibe (10 mg/day) was given to 17 patients with NAFLD for 6 months. The primary endpoint was change in serum aminotransferase level. Secondary outcomes were change in liver histology (12 control and 16 ezetimibe patients), insulin sensitivity including a hyperinsulinaemic–euglycaemic clamp study (ten control and 13 ezetimibe patients) and hepatic fatty acid composition (six control and nine ezetimibe patients). Hepatic gene expression profiling was completed in 15 patients using an Affymetrix gene chip. Patients and the physician in charge knew to which group the patient had been allocated, but people carrying out measurements or examinations were blinded to group.

Results Serum total cholesterol was significantly decreased in the ezetimibe group. The fibrosis stage and ballooning score were also significantly improved with ezetimibe treatment. However, ezetimibe treatment significantly increased HbA_{1c} and was associated with a significant increase in hepatic long-chain fatty acids. Hepatic gene expression analysis showed coordinate downregulation of genes involved in skeletal muscle development and cell adhesion molecules in the ezetimibe treatment group, suggesting a suppression of stellate cell development into myofibroblasts. Genes involved in the L-carnitine pathway were coordinately downregulated by ezetimibe treatment and those in the steroid metabolism pathway upregulated, suggestive of impaired oxidation of long-chain fatty acids.

Conclusions/interpretation Ezetimibe improved hepatic fibrosis but increased hepatic long-chain fatty acids and HbA_{1c} in patients with NAFLD. These findings shed light on previously unrecognised actions of ezetimibe that should be examined further in future studies.

Trial registration University Hospital Medical Information Network (UMIN) Clinical Trials Registry UMIN000005250.

Funding The study was funded by grants-in-aid from the Ministry of Education, Culture, Sports, Science and Technology, Japan, and research grants from MSD.

Keywords Ezetimibe · Fatty acid · Gene expression · Non-alcoholic fatty liver disease

Yumie Takeshita and Toshinari Takamura contributed equally to this work.

Electronic supplementary material The online version of this article (doi:10.1007/s00125-013-3149-9) contains peer-reviewed but unedited supplementary material, which is available to authorised users.

Y. Takeshita · T. Takamura (✉) · M. Honda · Y. Kita · K.-i. Kato · H. Misu · T. Ota · M. Nakamura · K. Yamada · H. Sunagozaka · K. Arai · T. Yamashita · E. Mizukoshi · S. Kaneko
Department of Disease Control and Homeostasis, Kanazawa University Graduate School of Medical Sciences, 13-1 Takara-machi, Kanazawa, Ishikawa 920-8641, Japan
e-mail: ttakamura@m-kanazawa.jp

Y. Zen
Histopathology Section, Institute of Liver Studies, King's College Hospital, London, UK

Abbreviations

ALT	Alanine aminotransferase
H-IR	Hepatic insulin resistance index
hsCRP	High-sensitivity C-reactive protein
ICG15	Indocyanine green retention rate at 15 min after venous administration
LXR	Liver-X-receptor
MCR	Glucose metabolic clearance rate
miR	MicroRNA
NAFLD	Non-alcoholic fatty liver disease
NAS	NAFLD activity score
NASH	Non-alcoholic steatohepatitis
NPC1L1	Niemann–Pick C1-like 1
PAI-1	Plasminogen activator inhibitor-1
RLP-C	Remnant-like particle cholesterol
sdLDL	Small dense LDL
SREBP	Sterol regulatory element binding protein
QUICKI	Quantitative insulin sensitivity check index

Introduction

Multiple metabolic disorders, such as diabetes [1], insulin resistance and dyslipidaemia [2], are associated with non-alcoholic fatty liver disease (NAFLD), ranging from simple fatty liver to non-alcoholic steatohepatitis (NASH). Steatosis of the liver is closely associated with insulin resistance. However, the toxic lipids are not intrahepatic triacylglycerols but, rather, it is non-esterified cholesterol [3, 4] and some NEFA [5] that contribute to inflammation and insulin resistance in hepatocytes.

The level of cholesterol is tightly regulated by endogenous synthesis in the liver and dietary absorption/biliary reabsorption in the small intestine. Niemann–Pick C1-like 1 (NPC1L1) plays a pivotal role in cholesterol incorporation in enterocytes [6]. Ezetimibe, a potent inhibitor of cholesterol absorption, inhibits NPC1L1-dependent cholesterol transport at the brush border of the intestine and the liver [6]. This suggests that ezetimibe ameliorates toxic-lipid-induced inflammation and insulin resistance by inhibiting cholesterol absorption. Indeed, ezetimibe improves liver steatosis and insulin resistance in mice [7] and Zucker obese fatty rats [8], although the beneficial effects of ezetimibe are observed only when the animals are fed a high-fat diet. Ezetimibe can also ameliorate liver pathology in patients with NAFLD [9, 10]; however, these studies lack a control group, which precludes meaningful conclusions as liver pathology can improve over the natural course of the disease or with tight glycaemic control in some NAFLD patients [1]. In the present study, we investigated the efficacy of ezetimibe treatment in patients with NAFLD for 6 months in an open-label randomised control study by examining liver pathology, as well as hepatic enzymes, glucose metabolism, hepatic fatty acid composition and hepatic gene expression profiles.

Methods

Patient selection Study staff recruited participants from outpatients at Kanazawa University Hospital, Ishikawa, Japan. Patients were recruited from April 2008 to August 2010, with follow-up visits during the 6 months thereafter. The study lasted from April 2008 to February 2011.

The inclusion criterion was a biopsy consistent with the diagnosis of NAFLD. Exclusion criteria included hepatic virus infections (hepatitis C virus [HCV] RNA–PCR-positive, hepatitis B and C, cytomegalovirus and Epstein–Barr virus), autoimmune hepatitis, primary biliary cirrhosis, sclerosing cholangitis, haemochromatosis, α_1-antitrypsin deficiency, Wilson's disease, history of parenteral nutrition and use of drugs known to induce steatosis (e.g. valproate, amiodarone and prednisone) or hepatic injury caused by substance abuse and/or the current or past consumption of more than 20 g of alcohol daily. None of the patients had any clinical evidence of hepatic decompensation, such as hepatic encephalopathy, ascites, variceal bleeding or an elevated serum bilirubin level more than twofold the upper normal limit.

A random allocation sequence was computer-generated elsewhere and assigned participants in a 1:1 ratio to treatment with ezetimibe or to the control group. All patients and responsible guardians underwent an hour of nutritional counselling by an experienced dietitian before starting the 6 month treatment period. The experienced dietitians were unaware of the study assignments. In addition, all patients were given a standard energy diet (125.5 kJ/kg per day; carbohydrate 50–60%, fat 20–30%, protein 15–20%) and exercise (5–6 metabolic equivalent estimations for 30 min daily) counselling before the study. Patients remained on stable doses of medications for the duration of the study. The patients in the ezetimibe group received generic ezetimibe (10 mg/day; Zetia, [Merck, Whitehouse Station, NJ, USA]) for 6 months.

The study was conducted with the approval of the Ethics Committee of Kanazawa University Hospital, Ishikawa, Japan, in accordance with the Declaration of Helsinki. Written informed consent was obtained from all individuals before enrolment. This trial is registered with the University Hospital Medical Information Network (UMIN) (Clinical Trials Registry, no. UMIN000005250).

Primary and secondary outcomes The primary endpoint was change in serum alanine aminotransferase (ALT) level at month 6 from baseline. Secondary outcomes included changes in the histological findings for NAFLD, hepatic gene expression profiling, fatty acid compositions of plasma and liver biopsy samples, lipid profiles, insulin resistance and

anthropometric measures, as well as assessment of ezetimibe safety. We had planned to enrol 80 patients in the trial, as we had estimated that with this sample size, the study would have 90% power at an α (two-tailed) value of 0.05 showing a 50% decrease of serum ALT values with 6 months of pioglitazone therapy on the basis of a previous study [11]. At the time of adverse event analyses, 32 of the targeted 80 patients had been randomly assigned and were included in the safety analyses.

Data collection Clinical information, including age, sex and body measurements, was obtained for each patient. Venous blood samples were obtained after the patients had fasted overnight (12 h) and were used to evaluate blood chemistry. Insulin resistance was estimated by HOMA-IR, calculated as [fasting insulin (pmol/l) × fasting glucose (mmol/l)]/22.5 [12] and insulin sensitivity was estimated as the quantitative insulin sensitivity check index (QUICKI)[13]. The adipose tissue insulin resistance index (adipose IR) was calculated as fasting NEFA (mmol/l)×fasting insulin (pmol/l) [14–16]. The indocyanine green retention rate at 15 min after venous administration (ICG15) was assessed using standard laboratory techniques before and after treatment. Serum fatty acids were measured with a gas chromatograph (Shimizu GC 17A, Kypto, Japan) at SRL (Tokyo, Japan).

Evaluation of insulin sensitivity derived from an OGTT After an overnight fast (10–12 h), a 75 g OGTT was performed at 08:30 hours. The OGTT-derived index of beta cell function, the insulinogenic index, computed as the suprabasal serum insulin increment divided by the corresponding plasma glucose increment in the first 30 min (ΔI30/ΔG30) [15, 17, 18] was calculated. From the OGTT data, the Matsuda index [19] was calculated. The hepatic insulin resistance index (H-IR) was calculated as the product of the total AUCs for glucose and insulin during the first 30 min of the OGTT (glucose 0–30 [AUC] [mmol/l]×insulin 0–30 [AUC] [pmol/l]). Skeletal muscle insulin sensitivity can be calculated as the rate of decline in plasma glucose concentration divided by plasma insulin concentration, as follows. Muscle insulin sensitivity index=dG/dt/mean plasma insulin concentration, where dG/dt is the rate of decline in plasma glucose concentration and is calculated as the slope of the least square fit to the decline in plasma glucose concentration from peak to nadir [20]. See the electronic supplementary material (ESM) for further details.

Evaluation of insulin sensitivity derived from the euglycaemic insulin clamp Insulin sensitivity in 23 of the 31 patients (10 control and 13 ezetimibe patients) was also evaluated in a hyperinsulinaemic–euglycaemic clamp study [21]. Patients did not receive any medication on the morning of the examination. At ~09:00 hours, after an overnight fast of at least 10 h, an intravenous catheter was placed in an antecubital vein in each individual for infusion, while a second catheter was placed in the contralateral hand for blood sampling. The euglycaemic–hyperinsulinaemic clamp technique was performed using an artificial pancreas (model STG-22; Nikkiso, Tokyo, Japan), as described previously [22]. See ESM for further details. The mean glucose metabolic clearance rate (MCR) in healthy individuals (n=9; age, 26.60± 2.9 years; body mass index, 22.3±2.1 kg/m^2) was 13.5± 3.4 mg kg^{-1} min^{-1} [2].

Liver biopsy pathology A single pathologist, who was blinded to the clinical information and the order in which the biopsies were obtained, analysed all biopsies twice and at separate times. The sections were cut from a paraffin block and stained with haematoxylin and eosin, Azan–Mallory and silver reticulin impregnation. The biopsied tissues were scored for steatosis (from 0 to 3), stage (from 1 to 4) and grade (from 1 to 3) as described [2], according to the standard criteria for grading and staging of NASH proposed by Brunt et al [23]. The NAFLD activity score (NAS) was calculated as the unweighted sum of the scores for steatosis (0–3), lobular inflammation (0–3) and ballooning (0–2), as reported by Kleiner et al [24].

Gene expression analysis of liver biopsied samples Gene expression profiling was performed in samples from nine patients in the ezetimibe group and six in the control group. Liver tissue RNA was isolated using the RNeasy Mini kit (QIAGEN, Tokyo, Japan) according to the manufacturer's instructions. See ESM for further details. Data files (CEL) were obtained using the GeneChip Operating Software 1.4 (Affymetrix). Genechip data analysis was performed using BRB-Array Tools (http://linus.nci.nih.gov/BRB-ArrayTools.html). The data were log-transformed ($\log_{10}$), normalised and centred. To identify genetic variants, paired t tests were performed to define p values <0.05 and fold change>1.5. Pathway analysis was performed using MetaCore (GeneGo, St Joseph, MI, USA). Functional ontology enrichment analysis was performed to compare the gene ontology (GO) process distribution of differentially expressed genes ($p<0.01$).

Fatty acid composition of liver Aliquots (0.2 mg) of liver samples snap-frozen by liquid nitrogen were homogenised in 1 ml normal NaCl solution (NaCl 154 mmol/l). Briefly, fatty acids were extracted by using pentadecanoic acid, and saponified with alkaline reagent (0.5 mmol/l KOH/ CH_3OH). The fatty acid methyl esters were analysed in a gas chromatograph (Shimadzu GC-2014 AF/SPL; Shimadzu Corporation, Kyoto, Japan) equipped with a flame ionisation detector and an auto injector. See ESM for further details. Mass spectra were analysed using GC solution (v. 2.3) software (Shimadzu Corporation, Kyoto, Japan, www.shimadzu.com). The changes in hepatic fatty acid composition are expressed as 10^{-4} mg/mg liver.

Statistical analysis Data are expressed as mean ± one standard error, unless indicated otherwise. The Statistical Package for the Social Sciences (SPSS; version 11.0; Chicago, IL, USA) was used for the statistical analyses. For univariate comparisons between the patient groups, Student's *t* test or Mann–Whitney's *U* test was used, as appropriate, followed by the Bonferroni multiple-comparison test. A value of $p < 0.05$ was considered to indicate statistical significance.

Results

Enrolment and discontinuation The data and safety monitoring board recommended that the study intervention and enrolment be discontinued because of the higher proportion of adverse events (significant elevation in HbA_{1c}) in the ezetimibe group than in the control group. At the time of adverse event analyses, 32 of the targeted 80 patients had been randomly assigned and were included in the safety analyses. In our open-label trial, 32 patients with NAFLD were enrolled. They were randomised to treatment with ezetimibe ($n=17$) or a control ($n=15$) with no significant clinical differences in variables between the groups. Of the 32 randomly assigned patients, 31 had completed the 6 month intervention period; one patient dropped out of the study. One case in the control group withdrew consent after randomisation and before intervention (ESM Fig. 1). The patient who withdrew was excluded from analysis because he did not start his course of treatment. Two analyses were conducted in the remaining patients. In the intention-to-treat analysis (ESM Tables 1 and 2), measures that were missing for participants who discontinued the study were replaced with baseline measures. In the second analysis, the only data included were from participants who completed the study to the end of the 6 month follow-up period. We performed a completed case analysis because there were few dropouts unrelated to baseline values or to their response.

Patient characteristics The 31 study patients (mean age 52.7±2.1 years; mean BMI 29.2±1.0) included 14 randomised to the control group and 17 to the ezetimibe group (ESM Table 3).

At baseline, the characteristics of patients in the ezetimibe and control groups were comparable except for the waist circumference ($p=0.085$) and the Matsuda index ($p=0.060$). The histological features of the liver are summarised in Table 1. At baseline, neither the severity of the individual histological features nor the proportion of patients distributed in the three NAS categories was significantly different between the two groups. All 31 participants agreed to complete the follow-up venous blood samples including OGTT. The ICG15 was conducted in 24 patients (ten control and 14 ezetimibe patients).

Changes in laboratory variables The primary study outcome, serum alanine aminotransferase levels, did not change after ezetimibe treatment (Table 2).

After 6 months of ezetimibe treatment, systolic blood pressure, HbA_{1c}, glycated albumin, and lathosterol were significantly increased, while total cholesterol levels, campesterol, sitosterol and ferritin were significantly decreased. In contrast, body weight, BMI, fasting plasma glucose, plasma γ-glutamyltransferase, triacylglycerols, HDL-cholesterol, small dense LDL (sdLDL), remnant-like particle cholesterol (RLP-C), type IV collagen 7 s levels, NEFA, total bile acid, high-sensitivity C-reactive protein (hsCRP), adiponectin, TNF-α, plasminogen activator inhibitor-1 (PAI-1), 8-isoprostanes and ICG15 did not change after ezetimibe treatment (Table 2). Adipose IR tended to increase in the ezetimibe group (from 88.1±25.5 to 107.5±25.5, $p=0.070$), but not in the control group.

When changes in the groups were compared, the ezetimibe group, but not the control group, had a significant decrease in total cholesterol (ezetimibe, −0.49±0.19 vs control, 0.06±0.14 mmol/l; $p=0.037$), whereas the ezetimibe group, but not control group, showed a significant elevation in HbA_{1c} (ezetimibe, 0.46±0.12% [4.95±1.28 mmol/mol] vs control, 0.08±0.13% [0.78±1.46 mmol/mol]; $p=0.041$). Also, there were significant differences between the groups in cholesterol and HbA_{1c} levels at 6 months. The multiple-comparison

Table 1 Histological characteristics of the livers of patients who completed the study at baseline and 6 months

Variable	Control		p^a	Ezetimibe		p^a	p^b
	Before	After		Before	After		
Steatosis	1.42±0.15	1.17±0.17	0.082	1.56±0.18	1.31±0.15	0.300	0.989
Stage	1.71±0.40	1.71±0.39	1.000	1.75±0.28	1.53±0.26	0.048	0.163
Grade	0.88±0.28	0.79±0.26	0.339	0.84±0.21	0.72±0.15	0.362	0.628
Acinar inflammation	0.88±0.20	0.83±0.20	0.674	1.00±0.13	0.97±0.13	0.751	0.060
Portal inflammation	0.67±0.19	0.71±0.13	0.795	0.44±0.16	0.56±0.16	0.333	0.941
Ballooning	0.58±0.23	0.58±0.23	1.000	0.69±0.20	0.41±0.15	0.045	0.677
NAFLD activity score	3.25±0.53	2.82±0.59	0.139	3.71±0.50	3.06±0.45	0.185	0.705

Data are expressed as the means ± SE

[a] p value for the intergroup comparison (baseline vs 6 month)

[b] p value for the intergroup comparison (changes from baseline between groups)

Table 2 Laboratory values, insulin sensitivity and insulin resistance derived from the euglycaemic insulin clamps and OGTTs of patients who completed the study at baseline and 6 months

Variable	Control			Ezetimibe			
	Before	After	p^a	Before	After	p^a	p^b
Male/female	9/5			11/6			0.232
Age (years)	55.5±3.0			50.4±2.9			
Body weight (kg)	74.4±6.2	73.0±5.6	0.144	81.5±4.6	80.1±4.2	0.367	0.983
BMI (kg/m^2)	27.7±1.7	27.3±1.5	0.172	30.5±1.2	30.0±1.1	0.383	0.999
Waist circumference (cm)	93.1±2.7	92.6±3.4	0.709	99.9±2.5	100.0±2.6	0.956	0.713
Systolic blood pressure (mmHg)	125.2±3.9	126.4±4.9	0.771	124.0±2.4	130.7±2.8	0.048	0.269
Fasting plasma glucose (mmol/l)	7.15±0.63	6.52±0.40	0.240	6.62±0.30	6.87±0.34	0.411	0.131
HbA_{1c} (%)	5.9±0.2	6.0±0.2	0.603	6.1±0.2	6.5±0.2	0.001	0.041
HbA_{1c} (mmol/mol)	40.8±2.2	41.6±2.6	0.603	43.0±2.6	48.0±2.3	0.001	0.041
Hepaplastin test (%)	115.9±5.8	117.1±6.4	0.624	113.7±4.6	111.8±3.7	0.583	0.459
Glycated albumin (%)	15.9±0.8	16.2±1.0	0.397	15.7±0.5	16.8±0.5	0.014	0.196
Serum aspartate aminotransferase (μkat/l)	31.1±4.4	30.3±3.0	0.780	41.8±6.7	33.7±4.1	0.252	0.365
Serum ALT (μkat/l)	37.9±6.8	38.0±4.5	0.978	53.2±8.6	49.3±6.5	0.683	0.723
Plasma γ-glutamyltransferase (μkat/l)	74.9±27.8	65.8±19.5	0.345	71.4±23.4	60.5±16.1	0.220	0.892
Total cholesterol (mmol/l)	5.14±0.21	5.20±0.18	0.672	5.14±0.20	4.65±0.17	0.024	0.037
Triacylglycerols (mmol/l)	1.34±0.12	1.17±0.12	0.105	1.43±0.11	1.46±0.13	0.857	0.303
HDL-C (mmol/l)	1.40±0.08	1.45±0.06	0.914	1.36±0.08	1.36±0.06	0.942	0.903
sdLDL (mmol/l)	0.52±0.07	0.54±0.07	0.782	0.61±0.10	0.50±0.06	0.201	0.251
RLP-C (mmol/l)	0.13±0.01	0.11±0.01	0.163	0.12±0.01	0.11±0.01	0.601	0.365
Lathosterol×10^{-3} (μmol/l)	2.27±0.43	2.85±0.52	0.001	3.52±0.52	5.01±0.67	<0.001	0.018
Campesterol×10^{-3} (μmol/l)	4.32±0.65	6.20±0.68	0.004	3.78±0.42	2.49±0.30	0.007	<0.001
Sitosterol×10^{-3} (μmol/l)	3.04±0.47	3.89±0.39	0.079	2.73±0.28	1.81±0.19	0.004	0.002
Ferritin (pmol/l)	412.1±85.6	235.3±47.0	0.009	395.7±81.3	247.8±56.8	0.005	0.689
Type IV collagen 7 s (μg/l)	4.52±0.48	4.42±0.45	0.622	4.23±0.23	4.33±0.20	0.592	0.465
NEFA (mmol/l)	0.50±0.09	0.63±0.06	0.160	0.51±0.05	0.57±0.03	0.835	0.447
Total bile acid (μmol/l)	12.5±8.0	8.8±5.2	0.214	5.0±0.7	4.8±1.3	0.893	0.267
hsCRP×10^{-3} (μg/ml)	0.12±0.02	0.09±0.02	0.050	0.14±0.04	0.13±0.04	0.886	0.767
Adiponectin (μg/ml)	4.0±0.5	4.6±0.8	0.114	3.0±0.6	3.3±0.6	0.299	0.670
TNF-α ×10^{-5} (pmol/ml)	10.4±2.3	15.6±8.1	0.094	8.1±0.6	30.0±12.7	0.183	0.084
Leptin×10^{-3} (μg/l)	8.1±1.0	9.7±1.3	0.044	10.8±1.4	12.4±1.5	0.085	0.982
PAI-1 (pmol/l)	400.0±44.2	436.5±44.2	0.401	550.0±71.2	488.5±67.3	0.217	0.136
8-Isoprostanes (pmol/mmol creatinine)	76.9±14.3	57.0±8.0	0.147	56.5±6.6	68.0±7.7	0.092	0.031
ICG15 (%)	8.7±2.4	8.5±2.0	0.662	7.7±1.7	7.7±1.5	0.984	0.796
HOMA-IR	10.1±6.5	5.0±2.1	0.471	9.5±2.6	9.3±2.2	0.839	0.479
QUICKI	0.32±0.01	0.33±0.01	0.443	0.30±0.01	0.30±0.01	0.984	0.019
Adipose IR	55.8±15.5	78.8±31.7	0.441	88.1±25.5	107.5±25.5	0.070	0.099
Insulinogenic index	0.43±0.09	0.53±0.11	0.307	0.41±0.08	0.35±0.09	0.501	0.765
H-IR×10^6	1.82±0.46	2.29±0.44	0.568	2.29±0.33	2.66±0.41	0.221	0.796
Matsuda index	3.03±0.45	3.35±0.49	0.368	1.99±0.28	2.01±0.29	0.895	0.013
Muscle insulin sensitivity	0.039±0.006	0.058±0.016	0.210	0.036±0.005	0.034±0.004	0.560	0.067
MCR	4.86±0.50	4.36±0.45	0.174	4.70±0.31	4.80±0.35	0.827	0.352

Data are expressed as means ± SE

[a] p value for the intergroup comparison (baseline vs 6 month)

[b] p value for the intergroup comparison (changes from baseline between groups)

HDL-C, HDL-cholesterol

Table 3 Signalling pathway gene expression changes in the ezetimibe group

Pathway	Gene symbol	Gene name	Affy ID	Up or down	Function
Development_skeletal muscle development	*VEGFA*	Vascular endothelial growth factor A	210512_s_at	Down	Angiogenesis
	ACTA2	Actin, α2, smooth muscle, aorta1	200974_at	Down	Cytoskeleton and cell attachment
	TCF3	Transcription factor 3	209153_s_at	Down	Differentiation
	TTN	Titin	1557994_at	Down	Abundant protein of striated muscle
	TPM2	Tropomyosin 2	204083_s_at	Down	Actin filament binding protein
	MYH11	Myosin, heavy chain 11, smooth muscle	201496_x_at	Down	Smooth muscle myosin
Immune response_phagocytosis	*FYB*	FYN-binding protein	205285_s_at	Up	Platelet activation and IL2 expression
	FCGR3A	Fc fragment of IgG, low affinity IIIA	204006_s_at	Up	ADCC and phagocytosis
	LCP2	Lymphocyte cytosolic protein 2	244251_at	Up	T cell antigen receptor mediated signalling
	CLEC7A	C-type lectin domain family 7, member A	221698_s_at	Up	T cell proliferation
	MSR1	Macrophage scavenger receptor 1	214770_at	Up	Macrophage-associated processes
	FCGR2A	Fc fragment of IgG, low affinity IIA	1565673_at	Up	Promotes phagocytosis
	PRKCB	Protein kinase C, β	209685_s_at	Up	B cell activation, apoptosis induction
	PLCB4	Phospholipase C, β4	240728_at	Up	Inflammation, cell growth, signalling and death
Cell adhesion_integrin priming	*GNA12*	G protein α12	221737_at	Down	Cytoskeletal rearrangement
	ITGB3	Integrin, β3	204628_s_at	Down	Ubiquitously expressed adhesion molecules
	PIK3R2	Phosphoinositide-3-kinase, regulatory subunit 2	229392_s_at	Down	Diverse range of cell functions
Cell adhesion_cadherins	*PTPRF*	Protein tyrosine phosphatase, receptor type, F	200636_s_at	Down	Cell adhesion receptor
	BTRC	β-Transducin repeat containing E3 ubiquitin protein ligase	222374_at	Down	Substrate recognition component of a SCF E3 ubiquitin-protein ligase complex
	CDHR2	Cadherin-related family member 2	220186_s_at	Down	Contact inhibition at the lateral surface of epithelial cells
	SKI	V-ski sarcoma viral oncogene homologue	229265_at	Down	Repressor of TGF-β signalling
	MLLT4	Myeloid/lymphoid or mixed-lineage leukaemia	214939_x_at	Down	Belongs to an adhesion system
	VLDLR	Very low density lipoprotein receptor	209822_s_at	Down	Binds VLDL and transports it into cells by endocytosis
O-Hexadecanoyl-L-carnitine pathway	*TUBB2B*	Tubulin, β 2B class IIB	209372_x_at	Down	Major component of microtubules
	TUBB2A	Tubulin, β2A class IIA	209372_x_at	Down	Major component of microtubules
	PLCE1	Phospholipase C, epsilon 1	205112_at	Down	Hydrolyses phospholipids into fatty acids and other lipophilic molecules
	CPT1B	Carnitine palmitoyltransferase 1B (muscle)	210070_s_at	Down	Rate-controlling enzyme of the long-chain fatty acid β-oxidation pathway
	CPT1A	Carnitine palmitoyltransferase 1A (liver)	203634_s_at	Down	Carnitine-dependent transport across the mitochondrial inner membrane
	NR1H4	Nuclear receptor subfamily 1, group H, member 4	243800_at	Down	Involved in bile acid synthesis and transport.
GalNAcbeta1-3Gal pathway	*PLCB4*	Phospholipase C, β4	240728_at	Up	Formation of inositol 1,4,5-trisphosphate and diacylglycerol
Steroid metabolism_cholesterol biosynthesis	*CYP51A1*	Cytochrome P450, family 51, subfamily A, polypeptide 1	216607_s_at	Up	Transforms lanosterol
	SREBF2	Sterol regulatory element binding transcription factor 2	242748_at	Up	Transcriptional activator required for lipid homeostasis
	SQLE	Squalene epoxidase	209218_at	Up	Catalyses the first oxygenation step in sterol biosynthesis

Table 3 (continued)

Pathway	Gene symbol	Gene name	Affy ID	Up or down	Function
	SC5DL	Sterol-C5-desaturase-like	215064_at	Up	Catalyses the conversion of lathosterol into 7-dehydrocholesterol
	HMGCS1	3-Hydroxy-3-methylglutaryl-CoA synthase 1	205822_s_at	Up	Condenses acetyl-CoA with acetoacetyl-CoA to form HMG-CoA

Bonferroni test revealed highly significant differences in the changes in total cholesterol ($p = 0.037$) and HbA_{1c} ($p = 0.040$) between the ezetimibe and control groups.

Increased concentrations of the cholesterol synthesis markers lathosterol (ezetimibe, 1.49±0.32 nmol/l vs control, 0.58±0.14 nmol/l; $p = 0.018$) and decreased concentrations of the cholesterol absorption markers campesterol (ezetimibe, −1.28±0.41 nmol/l vs control, 1.88±0.54 nmol/l, $p = 0.000$) and sitosterol (ezetimibe, −0.91±0.27 nmol/l vs control, 0.85± 0.45 nmol/l; $p = 0.002$) were observed on treatment. The ezetimibe group had an increase, whereas the control group had a decrease, in the level of 8-isoprostanes (ezetimibe, 11.6± 6.4 pmol/mmol creatinine vs control, −19.9±12.9 pmol/mmol creatinine; $p = 0.031$).

When changes between groups were compared, the ezetimibe group had a greater decrease in the Matsuda index (ezetimibe=−0.78±0.57 vs control=−1.35±0.55, $p = 0.013$), QUICKI (ezetimibe= −0.02±0.01 vs control=0.03±0.0, $p = 0.019$), and muscle insulin sensitivity (ezetimibe= −0.002±0.004 vs control=0.019±0.014, $p = 0.067$) than the control group.

Changes in liver histology Twenty-eight of 31 participants, 16 in the ezetimibe group and 12 in the control group, agreed to complete the follow-up and undergo a liver biopsy at 6 months, allowing for complete case analysis of the data (Table 1). After 6 months, the changes in staging score (from 1.75±0.28 to 1.53±0.26) and ballooning score (from 0.69± 0.20 to 0.41±0.15) were significantly improved in the ezetimibe group compared with the control group, whereas the scores of steatosis, lobular inflammation and NAS were not significantly changed in either group. The degree of all of these histological features was not significantly different between the two groups (Table 1).

Serial changes in liver gene with ezetimibe treatment Gene expression profiling was conducted in samples from nine patients in the ezetimibe group and six in the control group (ESM Table 4). In the ezetimibe group, 434 genes were upregulated and 410 genes downregulated, while in the control group, 643 genes were upregulated and 367 genes downregulated. Pathway analysis of the process network of differentially expressed genes showed coordinate downregulation of genes involved in skeletal muscle development and cell adhesion molecules in the ezetimibe group, suggesting a suppression of stellate cell development into myofibroblasts (Table 3). In addition, ezetimibe activated the immune response pathway. In contrast, genes involved in skeletal muscle development were upregulated and those in the immune response downregulated in the control group (Table 4). Pathway analysis of the metabolic network also revealed decreased L-carnitine pathway and increased steroid metabolism with ezetimibe treatment, but decreased CoA biosynthesis and increased glycerol 3-phosphate pathway in the control group (ESM Fig. 2).

Changes in plasma fatty acid composition and fatty acid composition extracted from liver tissue The changes in plasma fatty acid composition are shown in Table 5. Compared with baseline levels, only eicosatrienoic acid was significantly increased in the ezetimibe group.

Fatty acid composition in extracted liver tissue was available for 16 NAFLD patients treated with ezetimibe and 12 controls (Table 6). Ezetimibe treatment for 6 months significantly and markedly increased hepatic lauric, myristic, palmitic, palmitoleic, margaric and stearic acids compared with the control group. The changes in hepatic fatty acid composition did not correlate with the changes in serum fatty acid composition before and after ezetimibe treatment (ESM Table 5).

Discussion

This is the first report of the efficacy of ezetimibe treatment on liver pathology in patients with NAFLD in an open-label randomised controlled trial. Treatment with 10 mg/day ezetimibe for 6 months did not alter the primary study outcome, serum aminotransferase levels. Ezetimibe significantly decreased serum cholesterol levels and cholesterol absorption markers as expected, whereas, in contrast to previous reports, ezetimibe treatment did not decrease serum levels of triacylglycerol. Our initial hypothesis was that ezetimibe treatment ameliorates liver pathology by inhibiting the absorption of toxic lipids such as oxidised cholesterol and palmitate. In our animal model, cholesterol feeding to mice increased not

Table 4 Signalling pathway gene expression changes in the control group

Pathway	Gene symbol	Gene name	Affy ID	Up or down	Function
Muscle contraction	*MYH11*	Myosin, heavy chain 11, smooth muscle	201497_x_at	Up	Smooth muscle myosin
	CALM1	Calmodulin 1	241619_at	Up	Ion channels and other proteins by Ca^{2+}
	KCNJ15	Potassium inwardly-rectifying channel, subfamily J, member 15	211806_s_at	Up	Integral membrane protein, inward-rectifier type potassium channel
	SRI	Sorcin	208920_at	Up	Modulates excitation–contraction coupling in the heart
	ACTA2	Actin, α2, smooth muscle, aorta	215787_at	Up	Cell motility, structure and integrity
	TTN	Titin	1557994_at	Up	Abundant protein of striated muscle
	EDNRA	Endothelin receptor type A	204463_s_at	Up	Receptor for endothelin-1
	TPM2	Tropomyosin 2	204083_s_at	Up	Actin filament binding protein
	CRYAB	Crystallin, αB	209283_at	Up	Transparency and refractive index of the lens
Development_skeletal muscle development	*GTF2IRD1*	GTF2I repeat domain containing 1	218412_s_at	Up	Transcription regulator involved in cell-cycle progression, skeletal muscle differentiation
	ADAM12	ADAM metallopeptidase domain 12	213790_at	Up	Skeletal muscle regeneration
	MAP1B	Microtubule-associated protein 1B	226084_at	Up	Facilitates tyrosination of α-tubulin in neuronal microtubules
	MYOM1	Myomesin 1	205610_at	Up	Major component of the vertebrate myofibrillar M band
Cell cycle_G1-S growth factor regulation	*DACH1*	Dachshund homologue 1	205472_s_at	Up	Transcription factor that is involved in regulation of organogenesis
	FOXN3	Forkhead box N3	229652_s_at	Up	Transcriptional repressor, DNA damage-inducible cell cycle arrests
	TGFB2	Transforming growth factor, β2	228121_at	Up	Suppressive effects on interleukin-2 dependent T cell growth
	PIK3CD	Phosphatidylinositol-4,5-bisphosphate 3-kinase, catalytic subunit delta	203879_at	Up	Generate PIP3, recruiting PH domain-containing proteins to the membrane
	EGFR	Epidermal growth factor receptor	1565484_x_at	Up	Antagonist of EGF action
	CCNA2	Cyclin A2	203418_at	Up	Control of the cell cycle at the G1/S and the G2/M transitions
	AKT3	v-Akt murine thymoma viral oncogene homologue 3	219393_s_at	Up	Metabolism, proliferation, cell survival, growth and angiogenesis
	PRKD1	Protein kinase D1	205880_at	Up	Converts transient DAG signals into prolonged physiological effects
Regulation of metabolism_	*INSR*	Insulin receptor	226450_at	Down	Pleiotropic actions of insulin
Bile acid regulation of lipid metabolism and	*SLC27A5*	Solute carrier family 27, member 5	219733_s_at	Down	Bile acid metabolism
Negative FXR-dependent regulation of bile acids concentration	*MBTPS2*	Membrane-bound transcription factor peptidase	1554604_at	Down	Intramembrane proteolysis of SREBPs
	PIK3R3	Phosphoinositide-3-kinase, regulatory subunit 3	202743_at	Down	During insulin stimulation, it also binds to IRS-1
	MTTP	Microsomal triacylglycerol transfer protein	205675_at	Down	Catalyses the transport of triglyceride, cholesteryl ester, and phospholipid
	PPARA	Peroxisome proliferator-activated receptor α	226978_at	Down	Ligand-activated transcription factor
	CYP7A1	Cytochrome P450, family 7, subfamily A	207406_at	Down	Catalyses cholesterol catabolism and bile acid biosynthesis
	FOXA3	Forkhead box A3	228463_at	Down	Transcription factor

Table 4 (continued)

Pathway	Gene symbol	Gene name	Affy ID	Up or down	Function
Immune response_phagosome in antigen presentation	*HLA-B*	Major histocompatibility complex, class I, B	211911_x_at	Down	Foreign antigens to the immune system
	CD14	CD14 molecule	201743_at	Down	Mediates the innate immune response to bacterial lipopolysaccharide
	LBP	Lipopolysaccharide binding protein	211652_s_at	Down	Binds to the lipid A moiety of bacterial lipopolysaccharides
	CTSS	Cathepsin S	202901_x_at	Down	Thiol protease
	DERL1	Derlin 1	222543_at	Down	Functional component of endoplasmic reticulum-associated degradation
	CFL2	Cofilin 2	224352_s_at	Down	Reversibly controls actin polymerisation and depolymerisation
	PAK1	p21 protein (Cdc42/Rac)-activated kinase 1	230100_x_at	Down	Activated kinase acts on a variety of targets
Vitamin, mediator and cofactor	*SLC1A2*	Solute carrier family 1, member 2	1558009_at	Down	Transports L-glutamate and also L- and D-aspartate
Metabolism_CoA biosynthesis and transport	*PANK3*	Pantothenate kinase 3	218433_at	Down	Physiological regulation of the intracellular CoA concentration
	PANK1	Pantothenate kinase 1	226649_at	Down	Physiological regulation of the intracellular CoA concentration
	VNN1	Vanin 1	205844_at	Down	Membrane-associated proteins
	ACSL5	Acyl-CoA synthetase long-chain family member 5	222592_s_at	Down	Synthesis of cellular lipids and degradation via β-oxidation
	ACOT1	Acyl-CoA thioesterase 1	202982_s_at	Down	Catalyses the hydrolysis of acyl-CoAs to the NEFA and coenzyme A
	ACOT2	Acyl-CoA thioesterase 2	202982_s_at	Down	Catalyses the hydrolysis of acyl-CoAs to the NEFA and coenzyme A
	ENPP1	Ectonucleotide pyrophosphatase/ phosphodiesterase 1	229088_at	Down	Involved primarily in ATP hydrolysis at the plasma membrane
Phatidic acid pathway	*GPR63*	G protein-coupled receptor 63	220993_s_at	Up	Orphan receptor. May play a role in brain function
2-Oleoyl-glycerol_3-phosphate pathway	*LPAR1*	Lysophosphatidic acid receptor 1	204037_at	Up	Receptor for LPA, a mediator of diverse cellular activities

only cholesterol but also triacylglycerols in the liver, and upregulated the gene for sterol regulatory element binding protein (SREBP)-1c that governs fatty acid synthesis [3], probably via activation of liver-X-receptor (LXR) in the liver [25]. Therefore, in experimental models of high-cholesterol-diet-induced steatohepatitis, ezetimibe ameliorated liver steatosis by reducing cholesterol-induced activation of LXR and SREBP-1c [26, 27]. In the present study, however, treatment with ezetimibe unexpectedly ameliorated liver fibrosis staging and ballooning scores without significantly changing hepatic steatosis and insulin resistance.

One possible explanation for the improvement of hepatic fibrosis by ezetimibe treatment may be related to the direct effect of cholesterol on hepatic fibrogenesis. The cholesterol molecule affects membrane organisation and structure, which are critical determinants of membrane bilayer permeability and fluidity [28]. Altered cholesterol metabolism has several toxic effects on hepatocytes, resident macrophages, Kupffer cells and hepatic stellate cells, which promote NASH through diverse mechanisms. Hepatic stellate cells, in particular, are responsible for liver fibrosis in NASH. It has recently been reported that intracellular cholesterol accumulation directly activates hepatic stellated cells through a toll-like receptor-4-dependent pathway and triggers hepatic fibrosis [29]. These effects might be more evident in humans because, unlike rodents, where NPC1L1 is primarily expressed in the intestine, in humans *NPC1L1* mRNA is highly expressed both in the small intestine and liver. Therefore, ezetimibe is estimated to inhibit not only dietary and biliary cholesterol absorption through the small intestine, but also reabsorption of biliary cholesterol in the liver [30, 31]. Thus, ezetimibe may inhibit liver fibrosis by ameliorating

Table 5 Changes in plasma fatty acid composition

Fatty acid	Control		p^a	Ezetimibe		p^a	p^b
	Before	After		Before	After		
C12:0 (lauric acid)	1.9±0.5	1.2±0.2	0.177	2.3±0.6	2.1±0.5	0.753	0.301
C14:0 (myristic acid)	24.9±2.5	23.6±2.9	0.575	27.1±2.8	29.5±3.7	0.441	0.352
C16:0 (palmitic acid)	698.0±24.7	690.0±38.2	0.827	714.3±32.5	717.0±36.2	0.991	0.893
C16:1n-7 (palmitoleic acid)	68.6±6.5	72.5±9.6	0.643	62.4±5.0	69.9±6.2	0.219	0.721
C17:0 (margaric acid)	NE	NE		NE	NE		
C18:0 (stearic acid)	203.3±9.4	196.7±6.9	0.488	207.2±7.7	211.0±9.9	0.854	0.571
C18:1n-9 (oleic acid)	560.2±31.3	556.4±30.3	0.914	547.3±23.9	578.8±32.1	0.475	0.550
C18:2n-6 (linoleic acid)	745.8±26.3	750.6±34.4	0.910	735.8±34.2	713.5±31.4	0.558	0.629
C18:3n-6 (γ-linolenic acid)	9.8±1.3	9.2±1.0	0.506	9.8±0.9	11.1±1.5	0.402	0.300
C18:3n-3 (α-linolenic acid)	21.7±1.6	20.1±1.4	0.285	23.0±2.2	21.6±1.5	0.507	0.924
C20:0n-6 (arachidic acid)	7.0±0.4	6.9±0.3	0.671	7.2±0.2	7.0±0.3	0.410	0.642
C20:1n-9 (eicosenoic acid)	4.8±0.3	4.8±0.4	0.323	4.3±0.2	4.2±0.3	0.831	0.343
C20:2n-6 (eicosadienoic acid)	6.1±0.4	6.1±0.3	0.899	5.6±0.2	5.7±0.3	0.774	0.770
C20:3n-6 (dihomo-γ-linolenic acid)	36.6±3.0	37.3±2.8	0.784	36.5±2.4	40.6±3.7	0.247	0.438
C20:3n-9 (eicosatrienoic acid)	2.5±0.4	2.4±0.4	0.941	1.9±0.2	2.7±0.5	0.034	0.079
C20:4n-6 (arachidonic acid)	135.7±8.4	138.8±6.0	0.689	143.8±11.1	151.1±11.0	0.538	0.787
C20:5n-3 (eicosapentaenoic acid)	67.0±9.0	71.3±9.3	0.640	64.4±7.2	59.1±5.7	0.385	0.369
C22:0 (behenic acid)	16.6±0.8	18.3±1.0	0.035	17.1±0.8	17.9±1.3	0.623	0.468
C22:1n-9 (erucic acid)	1.6±0.1	1.3±0.1	0.066	1.3±0.1	1.3±0.1	0.914	0.170
C22:2n-6 (docosadienoic acid)	NE	NE		NE	NE		
C22:4n-6 (docosatetraenoic acid)	3.9±0.2	4.2±0.2	0.252	4.4±0.3	4.9±0.6	0.262	0.689
C22:5n-3 (docosapentaenoic acid)	20.0±1.4	20.7±1.7	0.657	20.7±1.7	21.5±1.7	0.839	0.887
C22:6n-3 (docosahexaenoic acid)	128.7±9.8	138.6±9.3	0.231	126.5±10.0	128.3±10.8	0.936	0.456
C24:1 (nervonic acid)	35.4±2.2	36.1±2.1	0.656	31.6±1.8	30.3±1.9	0.275	0.263

Data are expressed as means ± SE

[a] p value for the intergroup comparison (baseline vs 6 month)

[b] p value for the intergroup comparison (changes from baseline between groups)

NE, not estimated

cholesterol-induced activation of hepatic stellate cells in patients with NAFLD. This hypothesis was well supported by the hepatic gene expression profile induced by ezetimibe administration. Ezetimibe treatment coordinately downregulated genes involved in skeletal muscle development and cell adhesion molecules, suggesting that ezetimibe suppressed stellate cell development into myofibroblasts and thereby inhibited fibrogenesis.

Another important finding of the present study was that treatment with ezetimibe significantly deteriorated glycaemic control. Ezetimibe therapy also altered the hepatic profile of fatty acid components by significantly increasing hepatic levels of lauric, myristic, palmitic, palmitoleic, margaric, stearic, oleic and linoleic acids. Experimentally, palmitate induces interleukin-8 [32], endoplasmic reticulum stress, and c-Jun amino-terminal kinase activation and promotes apoptosis in the liver [5, 33, 34]. Lipid-induced oxidative stress and inflammation are closely related to insulin resistance [3, 5], which could be relevant to the ezetimibe-induced deterioration of glucose homeostasis. Indeed, urinary excretion of 8-isoprostanes was significantly increased in the ezetimibe group compared with the control, and showed significant negative correlation with insulin sensitivity indices such as the Matsuda index and QUICKI in the present study (ESM Table 6). Moreover, hepatic gene expression in the ezetimibe group showed coordinated upregulation of genes involved in the immune response compared with those in the control group, suggestive of oxidative stress caused by ezetimibe treatment.

Pathway analysis of the metabolic network showed unique metabolic changes in the ezetimibe group compared with the control group. In the control group, genes involved in the CoA-biosynthesis pathway were coordinately downregulated, and those in the glycerol-3 phosphate pathway coordinately upregulated, suggesting activated triacylglycerols biosynthesis. In the ezetimibe group,

Table 6 Changes in hepatic fatty acid composition

Fatty acid	Control		p^a	Ezetimibe		p^a	p^b
	Before	After		Before	After		
C12:0 (lauric acid)	7.7±1.2	15.2±5.6	0.219	6.3±1.8	18.8±4.7	0.019	0.494
C14:0 (myristic acid)	19.9±2.5	33.0±10.1	0.228	17.6±2.2	56.6±13.0	0.014	0.148
C16:0 (palmitic acid)	185.9±23.8	303.9±118.2	0.334	169.7±22.9	583.9±176.8	0.042	0.202
C16:1n-7 (palmitoleic acid)	24.2±4.5	37.3±13.4	0.362	22.3±4.3	51.9±13.2	0.031	0.368
C17:0 (margaric acid)	4.6±0.7	3.5±0.1	0.400	5.3±0.8	16.0±4.1	0.024	0.025
C18:0 (stearic acid)	45.9±4.4	54.4±8.9	0.283	56.0±7.1	125.1±30.2	0.017	0.042
C18:1n-9 (oleic acid)	166.4±25.1	250.2±91.6	0.367	173.9±30.6	381.9±84.3	0.017	0.288
C18:2n-6 (linoleic acid)	80.4±12.3	87.9±22.5	0.556	73.9±8.5	147.3±36.1	0.035	0.066
C18:3n-6 (γ-linolenic acid)	ND	ND		ND	ND		
C18:3n-3 (α-linolenic acid)	0.6±0.4	0.0±0.0	0.171	0.6±0.4	0.0±0.0	0.178	0.981
C20:0n-6 (arachidic acid)	ND	ND		ND	ND		
C20:1n-9 (eicosenoic acid)	5.5±1.1	4.7±1.9	0.639	5.7±1.0	13.1±4.8	0.170	0.168
C20:2n-6 (eicosadienoic acid)	ND	ND		ND	ND		
C20:3n-6 (dihomo-γ-linolenic acid)	ND	ND		ND	ND		
C20:3n-9 (eicosatrienoic acid)	ND	ND		ND	ND		
C20:4n-6 (arachidonic acid)	ND	ND		ND	ND		
C20:5n-3 (eicosapentaenoic acid)	ND	ND		ND	ND		
C22:0 (behenic acid)	ND	ND		ND	ND		
C22:1n-9 (erucic acid)	14.2±2.5	11.7±2.7	0.474	16.2±2.4	19.2±1.0	0.664	0.468
C22:2n-6 (docosadienoic acid)	2.8±1.0	1.8±1.0	0.433	22.3±0.7	62.3±2.9	0.176	0.152
C22:4n-6 (docosatetraenoic acid)	ND	ND		ND	ND		
C22:5n-3 (docosapentaenoic acid)	ND	ND		ND	ND		
C22:6n-3 (docosahexaenoic acid)	13.6±3.5	7.8±3.3	0.232	14.2±3.7	48.7±19.9	0.109	0.097
C24:1 (nervonic acid)	ND	ND		ND	ND		

The data are expressed as 10^{-4} mg/mg liver, means ± SE

[a] p value for the intragroup comparison (baseline vs 6 month)

[b] p value for the intergroup comparison (changes from baseline between groups)

ND, not determined

genes involved in the L-carnitine pathway, including *CPT1A,* were coordinately downregulated. A decreased L-carnitine pathway could be associated with reduced β-oxidation of palmitic acids in mitochondria, resulting in an increase in long-chain fatty acids (lauric, myristic, palmitic, palmitoleic, margaric, stearic, oleic and linoleic acids). Unbalanced fatty acid composition could induce oxidative stress and lead to insulin resistance in the ezetimibe group. In addition, genes involved in the cholesterol and NEFA biosynthesis, including *SREBF2*, were coordinately upregulated in the ezetimibe group (Table 3), probably as a result of deceased absorption of exogenous cholesterol. Upregulation of *SREBF2* potentially represses the expression of hepatocyte nuclear factor 4, which is required for *CPT1* transcription [35]. Moreover, recent reports have demonstrated that microRNA (miR)-33, encoded by an intron of *Srebp2* [36], inhibits translation of transcripts involved in fatty acid β-oxidation, including *CPT1* [37]. miR-33 is also implicated in decreased insulin signalling by reducing insulin receptor substrate-2 [38, 39]. Hepatic gene expression profiles may, to some extent, explain hepatic fatty acid composition and impaired glycaemic control in the ezetimibe group. These novel SREBP-2-mediated pathways in the gene expression network may be relevant to a recent report that a polymorphism in the *SREBF2* predicts incidence and the severity NAFLD and the associated glucose and lipid dysmetabolism [15]. These unique hypotheses should be confirmed in future in vitro and in vivo studies.

Our study has some limitations. First, the number of patients is relatively small because the data and safety monitoring board recommended that the study intervention and enrolment be discontinued in light of the higher proportion of adverse events in the ezetimibe group than in the control group. Second, our trial was a 6 month open-label study that resulted in subtle changes in liver pathology compared with previous reports [40]. Indeed, a 6 month duration may be too short a period to expect improvement of fibrosis, which is a slowly

progressive process [40]. Third, the average serum aminotransferase levels were lower than those in previous studies [9, 10], and most of the patients had mild steatosis, fibrosis and lower NAS at baseline before ezetimibe treatment. Serum ALT levels did not decrease with ezetimibe treatment in the present study, in contrast to the significant improvement reported previously [9, 10]. And finally, secondary outcomes are always at risk of false-positive associations. Therefore, we not only presented the changes in HbA_{1c} ($p=0.001$ for ezetimibe treatment and $p=0.041$ for the intergroup difference at the end of the study), but also showed the signature of hepatic fatty acid composition and hepatic gene expression profiles that support the hypothesis that ezetimibe increases HbA_{1c} and hepatic fatty acids contents possibly through the SREBP-2–miR33 pathway. No previous studies have raised this issue, which is worth investigating. The same mechanism may underlie a statin-induced deterioration of glucose tolerance, which remains a serious concern. Furthermore, the SREBP-2–miR33 pathway may raise a concern for a safety issue of combination therapy with ezetimibe and statins because these agents may additively upregulate *SREBF2* expression [41]. Future large-scale, long-duration studies involving more severely affected patients are required to determine the definite efficacy and risks of ezetimibe in the treatment of NAFLD.

In conclusion, the present study represents the first randomised controlled clinical trial of the efficacy of ezetimibe on liver pathology, energy homeostasis, hepatic fatty acid composition and hepatic gene expression profiles in patients with NAFLD. The lipid profile and liver histology of cell ballooning and fibrosis were significantly improved by ezetimibe treatment. However, our findings suggest an increase in oxidative stress, insulin resistance and HbA_{1c} on treatment with ezetimibe, which should be taken into consideration in NAFLD patients.

Acknowledgements We thank M. Kawamura (Kanazawa University Graduate School of Medical Sciences) for technical assistance.

Funding This work was supported by Grants-in-Aid from the Ministry of Education, Culture, Sports, Science and Technology, Japan, and research grants from MSD (to TT and SK).

Duality of interest The authors declare that there is no duality of interest associated with this manuscript.

Contribution statement YT designed the study, recruited the patients, analysed the data and wrote the manuscript. TT designed the study, recruited the patients, interpreted the data and edited the manuscript. MH analysed the hepatic gene expression profiles. YK performed the statistical analyses. YZ analysed all the biopsies. KK, HM and TO recruited the patients and collected the clinical information. HS, KA and TY performed the liver biopsies and histological examinations. MN performed the DNA chip experiments. KY and EM analysed the hepatic fatty acid compositions. SK initiated and organised the study. All authors contributed to the acquisition, analysis and interpretation of data and the drafting and editing of the manuscript. All of the authors approved the final version of the manuscript.

References

1. Hamaguchi E, Takamura T, Sakurai M et al (2010) Histological course of nonalcoholic fatty liver disease in Japanese patients: tight glycemic control, rather than weight reduction, ameliorates liver fibrosis. Diabetes Care 33:284–286
2. Sakurai M, Takamura T, Ota T et al (2007) Liver steatosis, but not fibrosis, is associated with insulin resistance in nonalcoholic fatty liver disease. J Gastroenterol 42:312–317
3. Matsuzawa N, Takamura T, Kurita S et al (2007) Lipid-induced oxidative stress causes steatohepatitis in mice fed an atherogenic diet. Hepatology 46:1392–1403
4. Marí M, Caballero F, Colell A et al (2006) Mitochondrial free cholesterol loading sensitizes to TNF- and Fas-mediated steatohepatitis. Cell Metab 4:185–198
5. Nakamura S, Takamura T, Matsuzawa-Nagata N et al (2009) Palmitate induces insulin resistance in H4IIEC3 hepatocytes through reactive oxygen species produced by mitochondria. J Biol Chem 29: 14809–14818
6. Garcia-Calvo M, Lisnock J, Bull HG et al (2005) The target of ezetimibe is Niemann-Pick C1-like 1 (NPC1L1). Proc Natl Acad Sci U S A 102: 8132–8137
7. Muraoka T, Aoki K, Iwasaki T et al (2011) Ezetimibe decreases SREBP-1c expression in liver and reverses hepatic insulin resistance in mice fed a high-fat diet. Metabolism 60:617–628
8. Deushi M, Nomura M, Kawakami A et al (2007) Ezetimibe improves liver steatosis and insulin resistance in obese rat model of metabolic syndrome. FEBS Lett 581:5664–5670
9. Yoneda M, Fujita K, Nozaki Y et al (2010) Efficacy of ezetimibe for the treatment of non-alcoholic steatohepatitis: an open-label, pilot study. Hepatol Res 40:613–621
10. Park H, Shima T, Yamaguchi K et al (2011) Efficacy of long-term ezetimibe therapy in patients with nonalcoholic fatty liver disease. J Gastroenterol 46:101–107
11. Promrat K, Lutchman G, Uwaifo GI et al (2004) A pilot study of pioglitazone treatment for nonalcoholic steatohepatitis. Hepatology 39:188–196
12. Matthews DR, Hosker JP, Rudenski AS et al (1985) Homeostasis model assessment: insulin resistance and beta-cell function from fasting plasma glucose and insulin concentrations in man. Diabetologia 28:412–419
13. Katz A, Nambi SS, Mather K et al (2000) Quantitative insulin sensitivity check index: a simple, accurate method for assessing insulin sensitivity in humans. J Clin Endocrinol Metab 85:2402–2410
14. Musso G, Cassader M, de Michieli F, Rosina F, Orlandi F, Gambino R (2012) Nonalcoholic steatohepatitis versus steatosis: adipose tissue insulin resistance and dysfunctional response to fat ingestion predict liver injury and altered glucose and lipoprotein metabolism. Hepatology 56:933–942
15. Musso G, Cassader M, Bo S, de Michieli F, Gambino R (2013) Sterol regulatory element-binding factor 2 (SREBF-2) predicts 7-year NAFLD incidence and severity of liver disease and lipoprotein and glucose dysmetabolism. Diabetes 62:1109–1120
16. Gastaldelli A, Cusi K, Pettiti M, Hardies J, Miyazaki Y, Berria R, Buzzigoli E, Sironi AM, Cersosimo E, Ferrannini E, Defronzo RA (2007) Relationship between hepatic/visceral fat and hepatic insulin resistance in nondiabetic and type 2 diabetic subjects. Gastroenterology 133:496–506
17. Musso G, Gambino R, Cassader M (2010) Lipoprotein metabolism mediates the association of MTP polymorphism with beta-cell dysfunction in healthy subjects and in nondiabetic normolipidemic patients with nonalcoholic steatohepatitis. J Nutr Biochem 21:834–840
18. Abdul-Ghani MA, Williams K, DeFronzo RA, Stern M (2007) What is the best predictor of future type 2 diabetes? Diabetes Care 30: 1544–1548

19. Matsuda M, DeFronzo RA (1999) Insulin sensitivity indices obtained from oral glucose tolerance testing: comparison with the euglycemic insulin clamp. Diabetes Care 22:1462–1470
20. Abdul-Ghani MA, Matsuda M, Balas B, DeFronzo RA (2007) Muscle and liver insulin resistance indexes derived from the oral glucose tolerance test. Diabetes Care 30:89–94
21. DeFronzo RA, Tobin JD, Andres R (1979) Glucose clamp technique: a method for quantifying insulin secretion and resistance. Am J Physiol 237:E214–E223
22. Nagai Y, Takamura T, Nohara E et al (1999) Acute hyperinsulinemia reduces plasma concentrations of homocysteine in healthy men. Diabetes Care 22:1004
23. Brunt EM, Janney CG, Di Bisceglie AM et al (1999) Nonalcoholic steatohepatitis: a proposal for grading and staging the histological lesions. Am J Gastroenterol 94:2467–2474
24. Kleiner DE, Brunt EM, van Natta M et al (2005) Nonalcoholic Steatohepatitis Clinical Research Network. Design and validation of a histological scoring system for nonalcoholic fatty liver disease. Hepatology 41:1313–1321
25. DeBose-Boyd RA, Ou J, Goldstein JL, Brown MS (2001) Expression of sterol regulatory element-binding protein 1c (SREBP-1c) mRNA in rat hepatoma cells requires endogenous LXR ligands. Proc Natl Acad Sci U S A 13:1477–1482
26. de Bari O, Neuschwander-Tetri BA, Liu M et al (2012) Ezetimibe: its novel effects on the prevention and the treatment of cholesterol gallstones and nonalcoholic fatty liver disease. J Lipids 2012:302847
27. Jia L, Ma Y, Rong S et al (2010) Niemann-Pick C1-Like 1 deletion in mice prevents high-fat diet-induced fatty liver by reducing lipogenesis. J Lipid Res 51:3135–3144
28. Musso G, Gambino R, Cassader M (2013) Cholesterol metabolism and the pathogenesis of non-alcoholic steatohepatitis. Prog Lipid Res 52:175–191
29. Teratani T, Tomita K, Suzuki T et al (2012) A high-cholesterol diet exacerbates liver fibrosis in mice via accumulation of free cholesterol in hepatic stellate cells. Gastroenterology 142:152–164
30. Altmann SW, Davis HR Jr, Zhu LJ et al (2004) Niemann-Pick C1 Like 1 protein is critical for intestinal cholesterol absorption. Science 303:1201–1204
31. Temel RE, Brown JM, Ma Y et al (2007) Hepatic Niemann-Pick C1-like 1 regulates biliary cholesterol concentration and is a target of ezetimibe. J Clin Invest 117:1968–1978
32. Joshi-Barve S, Barve SS, Amancherla K et al (2007) Palmitic acid induces production of proinflammatory cytokine interleukin-8 from hepatocytes. Hepatology 46:823–830
33. Pagliassotti MJ, Wei Y, Wang D (2007) Insulin protects liver cells from saturated fatty acid-induced apoptosis via inhibition of c-Jun NH2 terminal kinase activity. Endocrinology 148:3338–3345
34. Malhi H, Bronk SF, Werneburg NW, Gores GJ (2006) Free fatty acids induce JNK-dependent hepatocyte lipoapoptosis. J Biol Chem 281: 12093–12101
35. Gerin I, Clerbaux LA, Haumont O et al (2010) Expression of miR-33 from an SREBP2 intron inhibits cholesterol export and fatty acid oxidation. J Biol Chem 285:33652–33661
36. Louet JF, Hayhurst G, Gonzalez FJ et al (2002) The coactivator PGC-1 is involved in the regulation of the liver carnitine palmitoyltransferase I gene expression by cAMP in combination with HNF4 alpha and cAMP-response element-binding protein (CREB). J Biol Chem 277:37991–38000
37. Xuefen X, Hailing L, Huaixin D et al (2009) Down-regulation of hepatic HNF4_ gene expression during hyperinsulinemia via SREBPs. Mol Endocrinol 23:434–443
38. Horie T, Ono K, Horiguchi M et al (2010) MicroRNA-33 encoded by an intron of sterol regulatory element-binding protein 2 (Srebp2) regulates HDL in vivo. Proc Natl Acad Sci U S A 107:17321–17326
39. Fernández-Hernando C, Moore KJ (2011) MicroRNA modulation of cholesterol homeostasis. Arterioscler Thromb Vasc Biol 31:2378–2382
40. Musso G, Cassader M, Rosina F, Orlandi F, Gambino R (2012) Impact of current treatments on liver disease, glucose metabolism and cardiovascular risk in non-alcoholic fatty liver disease (NAFLD): a systematic review and meta-analysis of randomised trials. Diabetologia 55:885–904
41. Bennett MK, Seo YK, Datta S, Shin DJ, Osborne TF (2008) Selective binding of sterol regulatory element-binding protein isoforms and co-regulatory proteins to promoters for lipid metabolic genes in liver. J Biol Chem 6:15628–15637

SCIENTIFIC REPORTS

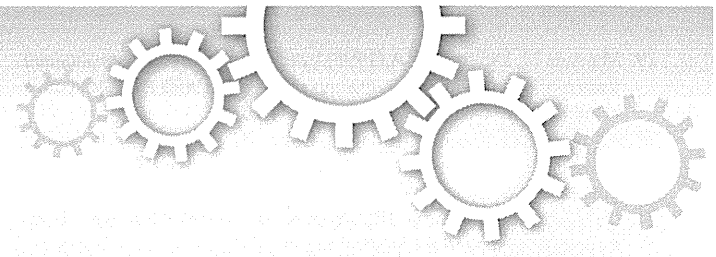

OPEN

SUBJECT AREAS:
HEPATITIS C VIRUS
DRUG REGULATION

Received
3 February 2014

Accepted
27 March 2014

Published
15 April 2014

Correspondence and requests for materials should be addressed to M.H. (mhonda@m-kanazawa.jp) or S.K. (skaneko@m-kanazawa.jp)

The Acyclic Retinoid Peretinoin Inhibits Hepatitis C Virus Replication and Infectious Virus Release *in Vitro*

Tetsuro Shimakami[1], Masao Honda[1], Takayoshi Shirasaki[1], Riuta Takabatake[1], Fanwei Liu[1], Kazuhisa Murai[1], Takayuki Shiomoto[1], Masaya Funaki[1], Daisuke Yamane[2], Seishi Murakami[1], Stanley M. Lemon[2] & Shuichi Kaneko[1]

[1]Department of Gastroenterology, Kanazawa University Hospital, Kanazawa, Ishikawa 920-8641, Japan, [2]Lineberger Comprehensive Cancer Center and the Division of Infectious Diseases, Department of Medicine, The University of North Carolina at Chapel Hill, Chapel Hill, NC 27599-7292, USA.

Clinical studies suggest that the oral acyclic retinoid Peretinoin may reduce the recurrence of hepatocellular carcinoma (HCC) following surgical ablation of primary tumours. Since hepatitis C virus (HCV) infection is a major cause of HCC, we assessed whether Peretinoin and other retinoids have any effect on HCV infection. For this purpose, we measured the effects of several retinoids on the replication of genotype 1a, 1b, and 2a HCV *in vitro*. Peretinoin inhibited RNA replication for all genotypes and showed the strongest antiviral effect among the retinoids tested. Furthermore, it reduced infectious virus release by 80–90% without affecting virus assembly. These effects could be due to reduced signalling from lipid droplets, triglyceride abundance, and the expression of mature sterol regulatory element-binding protein 1c and fatty acid synthase. These negative effects of Peretinoin on HCV infection may be beneficial in addition to its potential for HCC chemoprevention in HCV-infected patients.

Hepatitis C virus (HCV) is a causative agent of chronic hepatitis, liver cirrhosis, and hepatocellular carcinoma (HCC); therefore, the eradication of HCV from an infected liver could reduce death from HCV-related liver disease. Combination therapy of PEGylated-interferon (PEG-IFN) and ribavirin has long been the standard of care for patients with chronic hepatitis C (CH-C); however, a sustained viral response (SVR) is obtained in only ~50% of treated patients infected with genotype 1 HCV[1]. Recently, several classes of direct-acting antiviral agents (DAAs) have entered into clinical use. In the United States, two NS3/4A protease inhibitors, telaprevir and boceprevir, were approved for use in combination with PEG-IFN and ribavirin in 2011. Although the addition of these DAAs dramatically improves the SVR rate, 20–30% of patients still fail to eradicate HCV due to breakthrough by drug-resistant mutants or null response to therapy[2]. More potent DAAs are currently in late clinical development and promise much higher SVR rates even in the absence of PEG-IFN therapy; however, HCV-related HCC is likely to continue to be a significant clinical issue for many years because it will take time for potent DAAs to be distributed worldwide.

Peretinoin (generic name code: NIK-333) is an oral acyclic retinoid with a vitamin A-like structure that targets retinoid nuclear receptors, such as retinoid X receptor and retinoic acid receptor. The oral administration of Peretinoin significantly reduces the incidence of post-therapeutic HCC recurrence and improves the survival rate of patients in clinical trials[3,4]. In addition, Peretinoin prevents the development of hepatoma in several different hepatoma models[5,6]. Larger-scale clinical studies are currently ongoing in various countries to confirm its clinical efficiency. Depending on the results of these studies, Peretinoin may be used in CH-C patients to prevent HCC. Therefore, we sought to understand the effect of Peretinoin on HCV replication.

Peretinoin is categorised as a vitamin A or retinoid compound, and conflicting reports have described the effects of vitamin A compounds on HCV replication. One report showed that 3 retinoids, 9-cis retinoic acid (RA), 13-cis RA, and all-trans RA (ATRA), suppressed the replication of a sub-genomic HCV replicon[7]. However, vitamin A also reportedly enhances the replication of genome-length HCV in Huh-7 cells[8]. Here, we describe the impact of Peretinoin on different steps of the HCV life cycle, including translation, RNA amplification, virus assembly, and secretion, and its impact on host lipid metabolism *in vitro*. Our results clearly demonstrate that Peretinoin inhibits HCV RNA amplification and virus release by altering lipid metabolism.

Results

Inhibition of HCV RNA replication by retinoids. Several studies have tested the effects of vitamin A on HCV replication; these studies used a sub-genomic or full-genomic replicon, which contains 2 cistrons, one driven by HCV internal ribosome entry sites (IRES) and the other by encephalomyocarditis virus IRES[7,8]. We reported the usefulness of HCV genomes containing *Gaussia princeps* luciferase (GLuc) between p7 and NS2, followed by foot-and-mouth disease virus 2A, to monitor HCV RNA replication[9,10], and this system is closer to physiological HCV replication than the bicistronic replicon systems (Fig. 1A). In addition to GLuc-containing HCV genomes in the backbone of genotype 1a H77S.3, a chimeric clone of H77S and genotype 2a JFH1, HJ3-5[11], with structural proteins from H77S and non-structural proteins from JFH1, we also constructed GLuc-containing genomes in the backbone of genotype 1b N[12] and 2a JFH1[13] and confirmed their efficient replication in Huh-7.5 cells. Importantly, all of the strains used here are derived from cDNA clones that are infectious to chimpanzees.

We initially examined the effects of 4 different retinoids, namely ATRA, 9-cis RA, 13-cis RA, and Peretinoin, on HCV replication by using these 4 HCV genomes containing GLuc, according to the use of GLuc activity as an indicator of RNA replication, and the structures of each retinoid were shown in Supplementary Fig. S1 online. Peretinoin inhibited the replication of H77S.3/GLuc2A in a dose-dependent manner (Fig. 1B). As the other retinoids also suppressed HCV replication, we determined the antiviral half maximal effective concentrations (EC_{50}s) of these retinoids for each HCV genotype. Whilst Peretinoin showed the strongest antiviral effect on all genotypes tested, ATRA exerted a moderate effect, and 9-cis and 13-cis RA generated a weaker effect (Table 1). Especially, Peretinoin suppressed the RNA replication of H77S.3/GLuc2A most efficiently and its EC_{50} was 9 μM.

We also determined the half maximal cytotoxicity concentrations (CC_{50}s) of these retinoids in H77S.3/GLuc2A-replicating Huh-7.5 cells by using the WST-8 assay, which reflects cell number. The CC_{50}s of ATRA, 9-cis RA, and 13-cis RA were more than 100 μM; however, the CC_{50} of Peretinoin was 68 μM when the cells were treated for 72 h (Table 2). Although Peretinoin had a slightly negative impact on cell growth, as it showed the strongest antiviral effect and may be used for HCC chemoprevention in HCV-infected patients in the future, we focused upon the action of Peretinoin among these retinoids.

Inhibition of HCV RNA replication by Peretinoin. We examined the time dependence of the antiviral effect of Peretinoin. After HCV RNA transfection, we treated the transfected cells with Peretinoin at a range of concentrations (10–40 μM) and monitored RNA replication every 24 h until 72 h. Peretinoin started to show an antiviral effect from 24 h after treatment, which continued until 72 h. Peretinoin suppressed RNA replication in a time-dependent manner for all genotypes tested (Fig. 1C).

We also examined whether Peretinoin could also suppress RNA replication in a sub-genomic replicon system (Fig. 1D), in which infection should not occur due to the lack of structural proteins. Peretinoin was also able to suppress RNA replication in a dose-dependent manner in bicistronic sub-genomic RNA-transfected cells (Fig. 1E).

Importantly, when we treated HCV (H77S.3/GLuc2A)-replicating and HCV-non-replicating Huh-7.5 cells with Peretinoin at a range of concentrations (5–50 μM), the cell numbers were identical under the conditions tested (Fig. 1F).

As Peretinoin could suppress GLuc activity itself, we then examined directly its antiviral effect in the context of an HCV genome lacking the GLuc genome. For this purpose, Huh-7.5 cells infected with cell culture-derived HCV (HCVcc) of HJ3-5 were treated with different concentrations of Peretinoin. When we monitored HCV RNA replication by using quantitative real-time detection-polymerase chain reaction (RTD-PCR) (Fig. 2A) and protein expression by western blotting for the HCV core protein (Fig. 2B, see Supplementary Fig. S2 online), Peretinoin suppressed RNA replication and protein expression in a dose-dependent manner, which is consistent with the GLuc activity results. We also tested infectious virus production from Peretinoin-treated cells using a conventional focus forming unit (FFU) assay, and found that Peretinoin also reduced this in a dose-dependent manner (Fig. 2C).

Effect of Peretinoin on translation driven by HCV IRES. We also tested the effect of Peretinoin on translation directed by HCV IRES. For this purpose, we used a mini-genome RNA which has, sequentially, the HCV 5′-untranslated region (UTR), GLuc, and HCV 3′-UTR, and cap-*Cypridina* luciferase (CLuc)-polyA RNA as a control (see Supplementary Fig. S1 online). After we treated Huh-7.5 cells with different concentrations of Peretinoin for 24 h, we co-transfected the cells with these RNAs and measured GLuc and CLuc activity every 3 h from 3 to 12 h. When we normalised GLuc activity to CLuc activity at each time point, we did not observe a significant difference among the cells treated with the different concentrations of Peretinoin (see Supplementary Fig. S3 online), suggesting that Peretinoin does not have an effect on protein expression directed by HCV IRES.

Effect of Peretinoin on cellular interferon signalling. We hypothesised that the suppression of RNA replication by Peretinoin could be due to the activation or enhancement of cellular interferon (IFN) signalling. To examine this, we treated HCV (H77S.3/GLuc2A)-non-replicating and HCV-replicating Huh-7.5 cells with either IFNα-2b (10 IU/mL) or Peretinoin (10–40 μM) and monitored the expression of total and phosphorylated signal transducer and activator of transcription 1 (STAT1). Peretinoin did not alter the expression of either total or phosphorylated STAT1 in HCV-non-replicating Huh-7.5 cells or HCV-replicating cells (see Supplementary Fig. S4 online). In addition, Peretinoin did not further enhance the amount of phosphorylated STAT1 activated by IFNα-2b in HCV-non-replicating Huh-7.5 cells or HCV-replicating cells (see Supplementary Fig. S4 online). These data suggest that Peretinoin suppresses RNA replication without either activating or enhancing cellular IFN signalling.

Impact of Peretinoin on lipid metabolism. As lipid metabolism has an important role in various aspects of HCV infection[14–16], we examined the impact of Peretinoin on lipid metabolism. However, as it is sometimes difficult to detect small changes in lipid metabolism, we tested the effect of Peretinoin under oleic acid (OA) treatment, which amplifies changes in lipid metabolism. We treated H77S.3/GLuc2A-replicating Huh-7.5 cells with 40 μM Peretinoin and 250 μM OA, fixed and stained the cells with BODIPY 493/503 for lipid droplets (LDs) and 4′, 6-diamidino-2-phenylindole (DAPI) for nuclei, and used an anti-core protein antibody to detect HCV. When we stained LDs in the presence of 250 μM OA and the absence of Peretinoin, we observed intense signals (Fig. 3A); however, when it was accompanied with 40 μM Peretinoin, the signals from LDs were dramatically reduced, and at the same time, the expression of HCV core protein was also down-regulated (Fig. 3B). When we quantitated the signal strength from LDs and HCV core protein in 4 different fields, Peretinoin significantly reduced the signals from LDs and HCV core protein (two-tailed Student's t test, $p<0.0001$ for each) (Fig. 3C). This reduction was also confirmed by the quantitation of the 5 cells which were positive for both LDs and HCV core (see Supplementary Fig. S5 online). The reduced expression of HCV core protein was also observed by western blot analysis (Fig. 3D, see Supplementary Fig. S6 online). We next investigated the

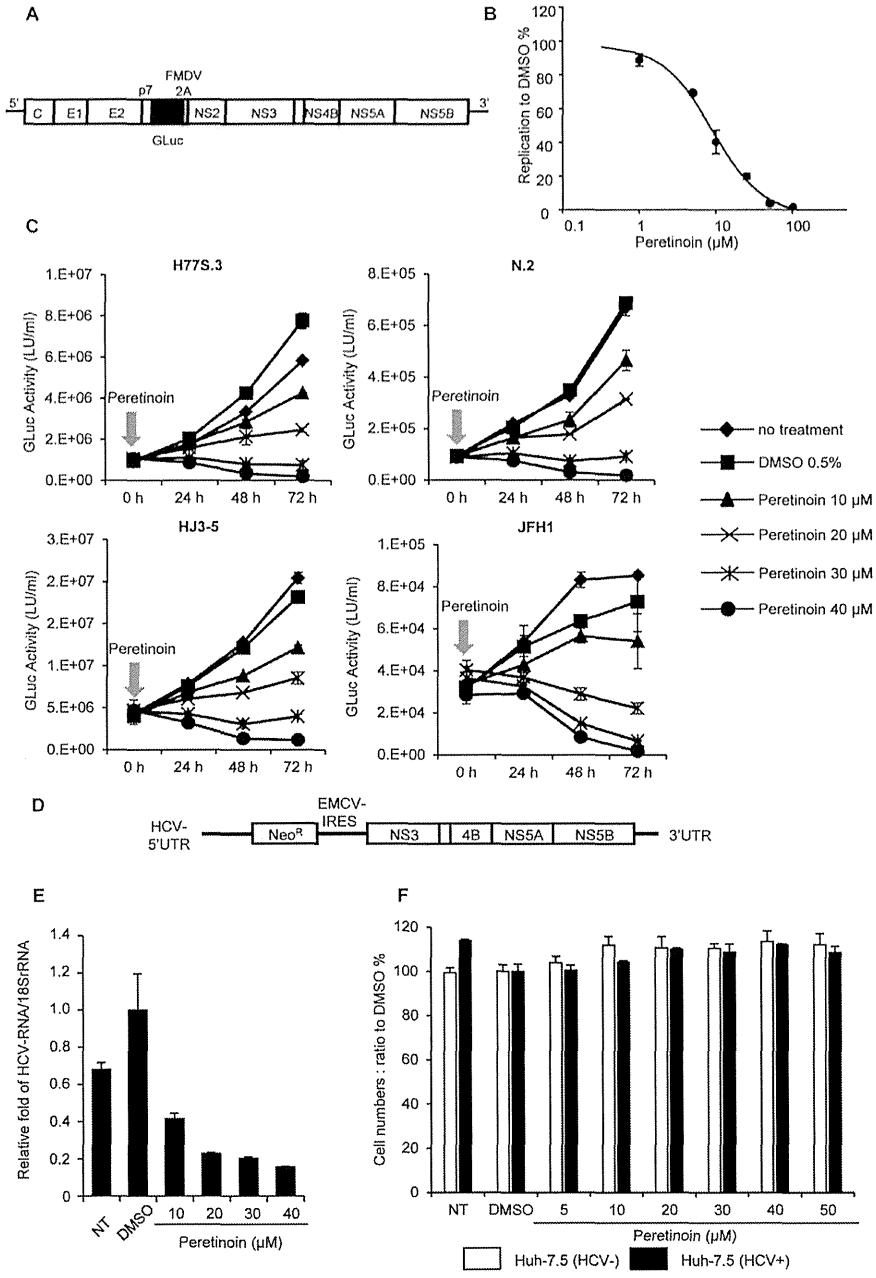

Figure 1 | Antiviral effects of several retinoids and their effects on cell growth. (A) Schematic representation of the GLuc-containing HCV genome. (B) Huh-7.5 cells were transfected with H77S.3/GLuc2A RNA, and 48 h later, 0.5% DMSO or Peretinoin was added at concentrations ranging from 1 to 100 μM. Fresh medium containing Peretinoin was added every 24 h, and 72 h after adding Peretinoin, secreted GLuc activity was measured. The GLuc activity from Peretinoin-treated cells was normalised to that with DMSO treatment. Data show the mean inhibition to DMSO treatment in each concentration of Peretinoin ± SD from 3 independent experiments. (C) Huh-7.5 cells were transfected with H77S.3/GLuc2A, N.2/GLuc2A, HJ3-5/GLuc2A, and JFH1/GLuc2A RNAs, and 48 h later, 0.5% DMSO or Peretinoin was added at the indicated concentrations. The medium was collected and replaced with fresh medium every 24 h until 72 h. GLuc activity was determined at each time point. The results shown represent the mean GLuc activity ± SD from 3 different plates. (D) Schematic representation of the bicistronic sub-genomic HCV RNA (E) Huh-7.5 cells were transfected with bicistronic sub-genomic RNA. At 48 h later, the transfected cells were treated with the indicated concentrations of Peretinoin for 72 h. Quantification of HCV RNA and 18S rRNA levels was performed and relative HCV RNA abundance normalised to the amount of 18S rRNA is presented as fold change ± SD compared to DMSO-treated cells from 3 independent experiments. (F) Huh-7.5 cells were transfected with H77S.3/GLuc2A RNA, and 7 days later, HCV (H77S.3/GLuc2A)-replicating Huh-7.5 cells, depicted as 'HCV+', were treated with the indicated concentrations of Peretinoin and HCV-non-replicating Huh-7.5 cells, depicted as 'HCV-', were also treated in a same way. At 72 h after Peretinoin treatment, cell numbers were determined by using a Cell Counting Kit-8. Data represent relative cell numbers ± SD from 3 independent experiments to DMSO-treated cells. EMCV, Encephalomyocarditis virus; Neo^R, Neomycin resistance gene; NT, no treatment.

Table 1 | EC_{50} of vitamin A compounds on HCV RNA replication

	Peretinoin		ATRA		9-cis RA		13-cis RA	
	Mean	SD	Mean	SD	Mean	SD	Mean	SD
HCV	(μM)	(μM)	(μM)	(μM)	(μM)	(μM)	(μM)	(μM)
H77S.3	9	1	32	3	29	7	41	4
N.2	19	1	53	5	75	8	83	17
HJ3-5	18	2	25	1	51	6	82	17
JFH1	20	1	25	1	61	8	78	11

impact of Peretinoin on lipid metabolism by measuring intracellular triglyceride (TG) levels, which should mainly reflect the amount of LDs, following treatment with 0–40 μM Peretinoin with or without HCV replication and OA treatment. Peretinoin reduced intracellular TG levels in a dose-dependent manner, regardless of OA treatment and HCV replication (Fig. 4A). These effects may be primarily due to its transcriptional modulation. To address this possibility, we examined the effect of Peretinoin on the transcription of fatty acid synthase (FASN) using RTD-PCR under 0–40 μM Peretinoin with or without HCV replication and OA treatment, because FASN is a key enzyme for the synthesis of fatty acids, which are an essential component of TGs. Peretinoin reduced the mRNA levels of FASN in a dose-dependent manner, regardless of OA treatment and HCV replication (Fig. 4B). We also examined FASN protein expression as well as the levels of precursor and mature sterol regulatory element-binding protein 1c (SREBP1c), which is a critical transcription factor for FASN. Peretinoin reduced the expression of FASN protein, which is consistent with the RTD-PCR results (Fig. 4C, see Supplementary Fig. S7 online). Although Peretinoin did not have an effect on precursor SREBP1c protein expression, it dramatically reduced the levels of mature SREBP1c (Fig. 4C, see Supplementary Fig. S7 online). We also observed a reduction of FASN mRNA levels by Peretinoin in an immortalised human hepatocyte cell line (Fig. 5A), and a similar reduction was also observed for ATRA, 9-cis RA, and 13-cis RA treatment of HCV-replicating Huh-7.5 cells (Fig. 5B). These results indicate that Peretinoin reduced intracellular lipid levels by reducing the amount of mature SREBP1c and, subsequently, FASN.

Specific inhibition of virus secretion by Peretinoin. Recently, lipids including LDs and TG have been reported to be important for efficient infectious virus production[14–16]. Due to its huge impact on lipid metabolism, Peretinoin could affect virus assembly or secretion as well as RNA amplification. To test the effect of Peretinoin on infectious virus production, we determined intra- and extra-cellular infectivity and the virus secretion ratio by measuring the amount of intra- and extra-cellular infectious virus from HJ3-5/GLuc2A-replicating FT3-7 cells treated with various concentrations of Peretinoin. We infected naïve Huh-7.5 cells with intra- and extra-cellular virus derived from HJ3-5/GLuc2A-replicating cells after Peretinoin treatment and used GLuc activity as an indicator of infectious virus production because FFUs and GLuc activity were well correlated (see Supplementary Fig. S8 online),

Table 2 | CC_{50} of vitamin A compounds on Huh-7.5 cells supporting HCV replication

Peretinoin		ATRA	9-cis RA	13-cis RA
Mean	SD	Mean	Mean	Mean
(μM)	(μM)	(μM)	(μM)	(μM)
68	5.2	>100	>100	>100

and a previous report also showed a good correlation between them[17]. Although Peretinoin did not show a significant impact on intracellular infectivity at 10–30 μM, it dramatically reduced extracellular infectivity and virus secretion from 10 μM when we normalised intra- and extra-cellular infectivity by the replication capacity of the virus producing the intra- and extra-cellular virus, as determined by GLuc activity (Fig. 6A). This result was also confirmed by using the extra-cellular virus which was prepared by centrifugation and subsequently re-suspended to fresh medium without containing Peretinoin, indicating that possible carryover of Peretinoin in the medium from extra-cellular cultures does not affect the result shown in Figure 6A (Supplementary Fig. S9 online). Interestingly, the expression of apolipoprotein E3 (ApoE3), which is essential for virus secretion, was also suppressed by Peretinoin (Fig. 4C, see Supplementary Fig. S7 online). Furthermore, we compared the buoyant density of HCVcc derived from HJ3-5/GLuc2A-replicating FT3-7 cells by equilibrium gradient ultracentrifugation. HCVcc from HJ3-5/GLuc2A-replicating cells treated with dimethyl sulfoxide (DMSO) or 30 μM Peretinoin showed exactly the same peak of infectivity at 1.107 g/cm^3 (Fig. 6B, 6C). Specific infectivity, as calculated from both peaks of HCV RNA and GLuc activity, was 0.0381 ± 0.0209 (standard deviation, SD) light units (LU)/copy for DMSO-treated cells, and 0.0799 ± 0.0457 LU/copy for Peretinoin-treated cells, which did not show a considerable difference. Furthermore, Peretinoin did not affect virus entry of HCVcc when we tested it by RT-PCR for HCV RNA at 5 h after infection and an FFU assay at 72 h after infection (see Supplementary Fig. S10 online). Collectively, Peretinoin seems to inhibit virus release in addition to viral RNA amplification.

Discussion

In the present study, we clearly showed that Peretinoin, as well as ATRA, 9-cis RA, and 13-cis RA, suppressed HCV RNA replication (Table 1). While previous reports used replicon systems to test the effects of retinoids, we used a genome-length HCV containing a GLuc-coding sequence between p7 and NS2, which is more physiological than replicons. The inhibitory effect of retinoids was universal among the HCV genotypes tested, and all retinoids tested showed an inhibitory effect on HCV replication (Table 1). In addition, we also observed the antiviral effect of Peretinoin in the replicon system (Fig. 1E). Therefore, our present data strongly support the notion that retinoids exert an antiviral effect *in vitro*. The antiviral effect of retinoids has also been confirmed in a clinical study. Even when CH-C patients were treated with ATRA, the viral load dropped by 1–2 log units in 50% of the patients enrolled. In addition, when CH-C patients who showed no response to prior IFN/PEG-IFNα and ribavirin therapy were treated with a combination of ATRA and PEG-IFNα-2a, 30% of patients showed a significant viral reduction[18]. Recently, combined vitamin A and D deficiency prior to IFN-based therapy was shown to be a strong independent predictor of non-response to antiviral therapy[19]. Collectively, our data and the clinical findings indicate that retinoids possess inhibitory effects on HCV replication.

Peretinoin showed the strongest antiviral effect among the retinoids tested (Table 1); thus, we focused on Peretinoin to clarify its antiviral mechanism. A previous report showed that 9-cis RA enhanced the antiviral effect of IFNα by increasing the expression of the IFNα receptor[20]; however, another study showed that ATRA did not induce the activation of dsRNA-activated protein kinase R, which is a key player in the IFN-induced antiviral response[7]. In the present study, Peretinoin did not increase the amount of the activated form of STAT-1, which is pSTAT1, contrary to IFNα-2b, both in HCV-replicating and HCV-non replicating Huh-7.5 cells, and dual treatment of Huh-7.5 cells with IFNα-2b and Peretinoin did not show a further increase of the pSTAT1 levels induced by only IFNα-2b (see Supplementary Fig. S4 online), indicating that

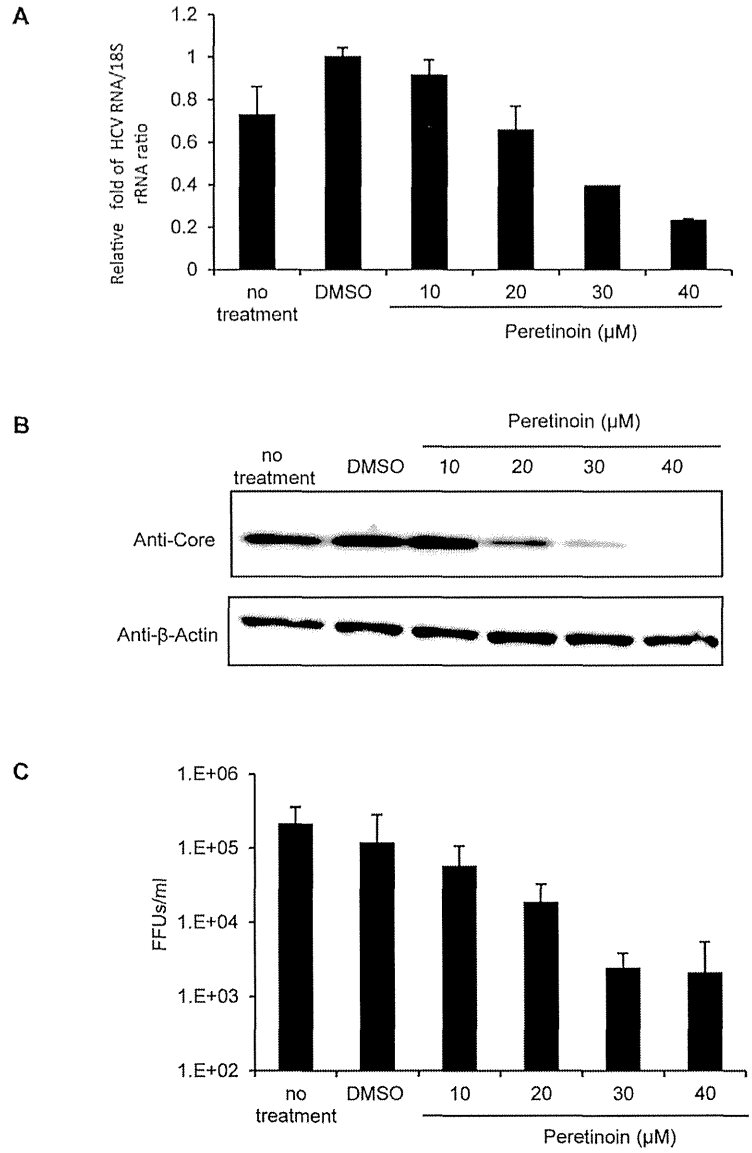

Figure 2 | Inhibition of HCV replication and infectious virus production. Huh-7.5 cells were infected with the HJ3-5 virus at a multiplicity of infection (MOI) of 1, and 72 h later, DMSO or Peretinoin was added at the indicated concentrations. The medium was replaced with fresh medium every 24 h until 72 h. (A) At 72 h after adding Peretinoin, total cellular RNA was extracted, and the amount of HCV RNA and 18S rRNA was quantitated by RTD-PCR. Relative HCV RNA abundance normalised to the amount of 18S rRNA is presented as fold change ± SD compared to DMSO-treated cells from 3 independent experiments. (B) At 72 h after Peretinoin treatment, the cell lysates were collected and subjected to western blot analysis using anti-core protein and anti-β-actin antibodies. Full-length blots/gels are presented in Supplementary Fig. S2 online. (C) The medium was collected at 72 h after Peretinoin treatment, and immediately, naïve Huh-7.5 cells were infected with serially diluted medium. At 72 h after infection, the infectious virus titre of HCVcc from Peretinoin-treated cells was determined by an FFU assay. Data shown here represent the mean FFUs/mL ± SD from 2 independent experiments.

Peretinoin did not activate or enhance cellular IFN signalling. Our results also indicate that the antiviral effect of Peretinoin is not due to the suppression of HCV translation directed by HCV IRES (see Supplementary Fig. S3 online). As Peretinoin suppressed the RNA replication of bicistronic sub-genomic replicons (Fig. 1E), it seems to suppress RNA amplification itself (see also the later description of FASN). A report showed that retinoids inhibited HCV RNA replication by enhancing the expression of gastrointestinal-glutathione peroxidase (GI-GPx) only in the presence of sodium selenite[7]; however, in the present study, we demonstrated that all retinoids tested inhibited HCV replication, even in the absence of sodium selenite. Thus, our results support the notion that the observed antiviral effects could be independent of GI-GPx, although supplementation with sodium selenite may further enhance the antiviral effects of retinoids.

To clarify the mechanism underlying the antiviral effect of Peretinoin further, we focused on the effect of Peretinoin on lipid metabolism because it has been shown to modify multiple aspects of HCV infection[14–16], and we detected a significant reduction of FASN

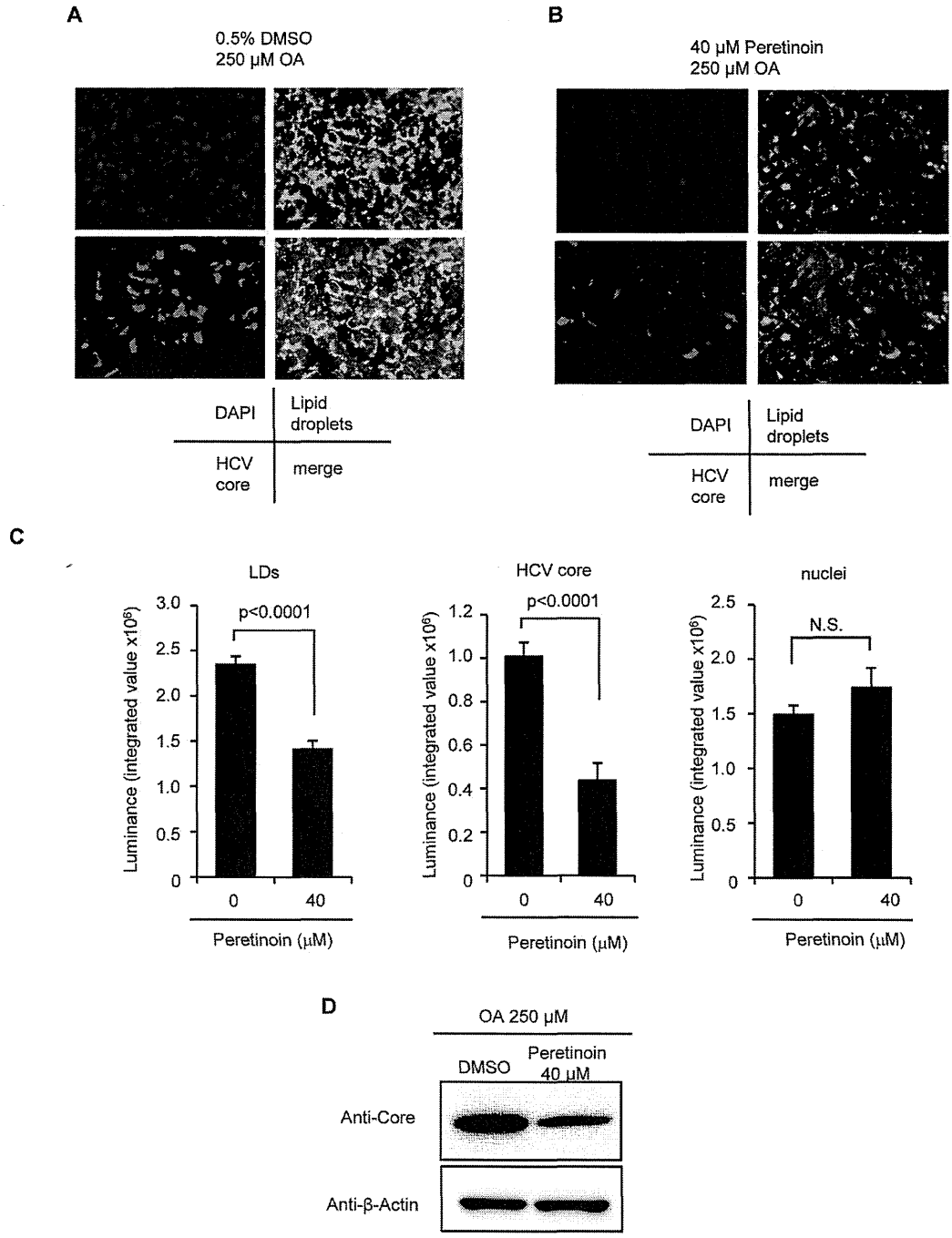

Figure 3 | Reduction of LD signals by Peretinoin. Huh-7.5 cells were infected with HJ3-5 virus at an MOI of 1, and 72 h later, 250 μM OA and DMSO or 250 μM OA and 40 μM Peretinoin were added, and the following assay was performed at 72 h later. (A, B) At 72 h later, the cells were fixed and stained for nuclei, LDs, and HCV core protein. (A) Shows 250 μM OA and DMSO-treated cells and (B) shows 250 μM OA and 40 μM Peretinoin-treated cells. The photos in (A) and (B) were taken under exactly the same conditions. (C) The signal intensity from LDs, HCV core protein, and nuclei was quantitated as described in the Methods. Data shown represent mean signal intensity ± SD from 4 different areas, and the difference was analysed statistically using Student's t-test. (D) Cell lysates were collected and subjected to western blot analysis using anti-core protein and anti-β-actin antibodies. Full-length blots/gels are presented in Supplementary Fig. S6 online. N.S., not significant.

mRNA levels by Peretinoin in a mouse hepatoma model, implying its possible effect on lipid metabolism[5]. Surprisingly, Peretinoin strongly reduced the signal from LDs in the presence of OA and intracellular TGs (Fig. 3A–C, 4A). LDs are known to have an essential role in the assembly of HCV virus particles by interacting with HCV core protein and NS5A[21,22]. Therefore, we examined the effect of Peretinoin on several steps of infectious virus production, such as assembly and secretion. Interestingly, Peretinoin specifically